Editors' Suggestion | Featured in Physics

Observation of Chemical Reactions between a Trapped Ion and Ultracold Feshbach Dimers

H. Hirzler,[1] R. S. Lous,[1] E. Trimby,[1] J. Pérez-Ríos,[2,3,4] A. Safavi-Naini,[5,6] and R. Gerritsma[1,5]
[1]Van der Waals-Zeeman Institute, Institute of Physics, University of Amsterdam, 1098 XH Amsterdam, The Netherlands
[2]Fritz-Haber-Institut der Max-Planck-Gesellschaft, Faradayweg 4-6, 14195 Berlin, Germany
[3]Institute for Molecules and Materials, Radboud University, Heyendaalseweg 135, 6525 AJ Nijmegen, The Netherlands
[4]Department of Physics and Astronomy, Stony Brook University, Stony Brook, New York 11794, USA
[5]QuSoft, Science Park 123, 1098 XG Amsterdam, The Netherlands
[6]Institute for Theoretical Physics, Institute of Physics, University of Amsterdam, Science Park 904, 1098 XH Amsterdam, The Netherlands

(Received 27 October 2021; accepted 1 February 2022; published 10 March 2022)

We measure chemical reactions between a single trapped $^{174}Yb^+$ ion and ultracold Li_2 dimers. This produces $LiYb^+$ molecular ions that we detect via mass spectrometry. We explain the reaction rates by modeling the dimer density as a function of the magnetic field and obtain excellent agreement when we assume the reaction to follow the Langevin rate. Our results present a novel approach towards the creation of cold molecular ions and point to the exploration of ultracold chemistry in ion molecule collisions. What is more, with a detection sensitivity below molecule densities of 10^{14} m^{-3}, we provide a new method to detect low-density molecular gases.

DOI: 10.1103/PhysRevLett.128.103401

Introduction.—To identify how quantum effects contribute to physical and chemical processes, it is essential to study chemical reactions at very low temperatures where only few partial waves play a role. Ion-molecule mixtures present a versatile platform to measure reaction channels with increased richness as compared to atomic mixtures. Interacting ions and molecules have been studied by letting ions collide with molecules from the vacuum background [1–3], from inlet room-temperature sources [4] and from molecular beams [5–7]. In these studies molecule temperatures were in the 1 K range, which is far above the ion-molecule *s*-wave collision energies. However, molecular samples of much lower temperatures can be created from ultracold atoms using Feshbach resonances [8–10]. These weakly bound diatomic molecules are called Feshbach dimers. Merging the fields of trapped ions and ultracold quantum gases [11] paves the way for studying ion-molecule collisions in the ultracold regime.

An important premise to control ion-neutral interactions in the ultracold regime is the understanding of the relevant reaction channels. Examples are charge transfer [12–15], spin exchange [16–18], and three-body recombination [19–22]. The exceptional control over the quantum states of trapped ions [23,24] makes it possible to study these chemical reactions at the single particle level and gives direct experimental access to the reaction products, their quantum states and energies, as well as their branching ratios. Single trapped ions can thus be used as probes to detect properties of the ultracold gases in which they are immersed [15,25]; e.g., BEC-BCS crossover regime [26] and the charged polarons [11,27–29]. Moreover, ultracold molecule-ion mixtures can be used to form cold molecular ions with applications in quantum information and precision spectroscopy [30–35]

In this Letter, we report on the observation of cold collisions between single Yb^+ ions in a Paul trap and a mixture of ultracold Li atoms and Li_2 dimers. We study the occurence of chemical reactions by observing the Yb^+ fluorescence after it has interacted with the cloud, counting the number of times the Yb^+ ion goes dark. We measure a negative correlation between the dark events probability and the atom density, indicating that atoms are not involved. Instead, we find that the reaction $Li_2 + Yb^+ \rightarrow LiYb^+ + Li$ leads to the dark events. We use mass spectrometry to demonstrate the occurrence of $LiYb^+$ molecular ions. We show excellent agreement between the probability of dark events and the Li_2 density in our system, which we model with rate equations. We use our ion sensor to detect about 50 dimers in a cloud of $\sim 10^4$ atoms, which provides a new tool to detect molecules in sparse quantities. This creates a pathway to create cold molecular ions and to search for quantum effects in ion-molecule collisions. Using ultracold Feshbach dimers, our molecules are 2–5 orders of magnitude colder compared to previous ion-molecule studies [1–7].

Experimental sequence.—The Yb^+-Li mixture is prepared in a hybrid ion-neutral trap as depicted in Fig. 1 and more extensively described in Ref. [36]. We load a single $^{174}Yb^+$ ion by isotope-selective two-photon ionization, Doppler-cool it to about 0.5 mK and prepare it in the

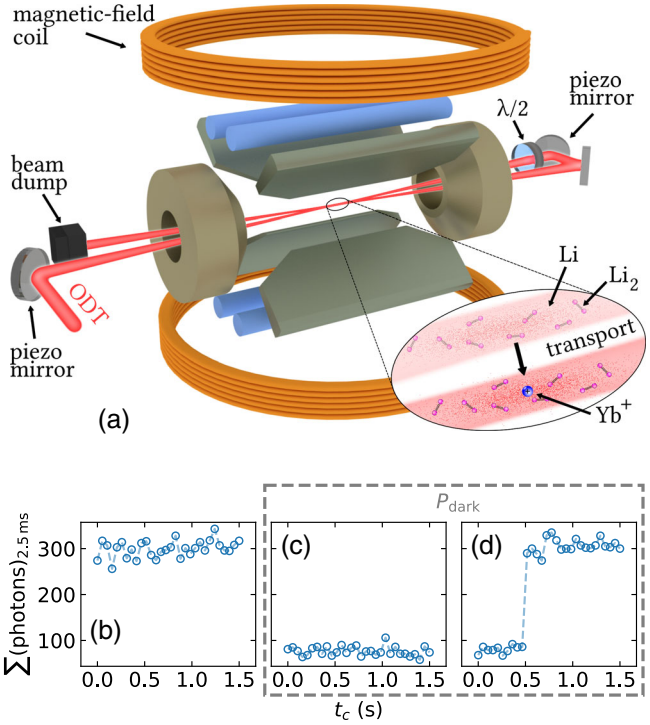

FIG. 1. Experimental setup with optical dipole trap (ODT) and Paul trap (shown in gray) to confine atoms and single ions respectively. The lower panel shows single-run Yb^+ ion 2.5 ms fluorescence detection versus time after ion-bath interaction resulting in (b) a bright Yb^+, (c) a lost Yb^+, and (d) a Yb^+ that turns bright after $t_c \approx 0.5$ s of Doppler cooling.

$^2S_{1/2}$ ground state. The ion trap operates at a driving frequency $\Omega = 2\pi \times 1.85$ MHz and trap frequencies $(\omega_x, \omega_y, \omega_z) \approx 2\pi \times (191, 196, 112)$ kHz, where z is the direction along the axis of the Paul trap. The ultracold fermionic Li atoms are prepared in a crossed 1070 nm, 40 μm waist, optical dipole trap (ODT) about 200 μm below the ion, using forced evaporative cooling at 663 G close to the 832 G Feshbach resonance [37]. We obtain about 2.2×10^4 ^{6}Li atoms per spin state in the lowest two magnetic sublevels $|F = 1/2, m_F = \pm 1/2\rangle$ at a temperature $T = 1$–10 μK. Here F is the total angular momentum quantum number and m_F is its projection on the quantization axis.

We admix a small quantity of Li_2 dimers to the bath by setting the magnetic field to $B_{Li_2} = 693$ G and associating the dimers by three-body recombination through direct evaporation. We do this in the final stage of the evaporation of the lithium spin mixture. The number of resulting dimers depends primarily on the temperature, the magnetic field B_{Li_2}, and the atom density n_a [38,39], which influences the three-body recombination and dissociation rate of the $Li + Li' + Li \rightleftharpoons Li_2 + Li$ reactions. Here, Li and Li′ indicate the two spin states. Next, we turn off the magnetic field, which increases the dimer binding energy to a fixed value of about $E_b/h = 1.38$ GHz [10,40], with h being Planck's constant. By ramping to zero field we minimize variations in the molecular ion formation rate [41], as well as quantum effects [11,51]. Moreover, as the binding energy (≈70 mK) is much greater than the dimer-ion collision energy, molecular ion formation is expected to be the dominant reaction channel [41]. For all the reported experiments we obtain dimer densities that are less than 10% of the atomic density. We measure the atom observables by time-of-flight absorption imaging.

We overlap the Yb^+ ion with the atom-dimer bath by transporting the ODT to the location of the Yb^+ ion by means of piezoelectric mirrors and let the systems interact for $\tau = 500$ ms. The interaction time was chosen to have sufficient contrast, yet reasonable experimental cycle time. Subsequently, we Doppler cool the Yb^+ ion for 1500 ms and simultaneously use a photomultiplier tube (PMT) to detect its fluorescence in time bins of 50 ms.

From the PMT measurements after the interaction, we identify three possible outcomes for each experimental run, as is indicated in Figs. 1(b)–1(d). After the interaction the Yb^+ ion is either bright [panel (b)] or dark [panel (c)] indicating ion loss. The final scenario occurs when the ion is initially dark, but after some cooling time t_c, it turns bright [panel (d)]. We count events (c) and (d) together as the dark ion probability P_{dark}.

The dark events hint towards the possibility of molecular ions being formed, as they resemble what was recently seen in the Ba^+-Rb system [22]. There, the photodissociation of the $BaRb^+$ molecular ion with light at 1064 nm, resulted in the observation of dark Ba^+ ions with similar fluorescence characteristics as panel (d). We will show that molecular ions in our system originate from ion-dimer collisions, via $Li_2 + Yb^+ \rightarrow LiYb^+ + Li$ as it was proposed in Ref. [41] in contrast to three-body recombination of molecular ions reported in Ref. [22].

Results.—We study the ion interacting with the atom-dimer bath and find a negative correlation between the probability of dark ions and the atom density, as shown in Fig. 2. In (a) we plot P_{dark} as a function of the ODT laser power P_{ODT} at the end of the evaporation ramp. The latter changes the peak atom density (5–0.5×10^{16} m^{-3}), presented in (b), as well as the temperature of the atom cloud (12–0.5 μK) and the dimer density [40].

Additional charge exchange measurements of the process $Yb^+(^2P_{1/2}) + Li \rightarrow Li^+ + Yb$ are taken as an independent means to probe the atomic density [see Fig. 2(c)]. Charge exchange occurs when we laser excite the ion to the $^2P_{1/2}$ state during the interaction with the bath and it directly leads to ion loss [15]. To avoid signal saturation we use $\tau = 50$ ms. Since the charge exchange rate is independent of the collision energy, its rate is a direct probe of the local atom density around the ion. The measurements confirm the trend observed in Fig. 2(b).

The negative correlation between P_{dark} and n_a, excludes Li atoms as the origin for the reaction resulting in P_{dark} and

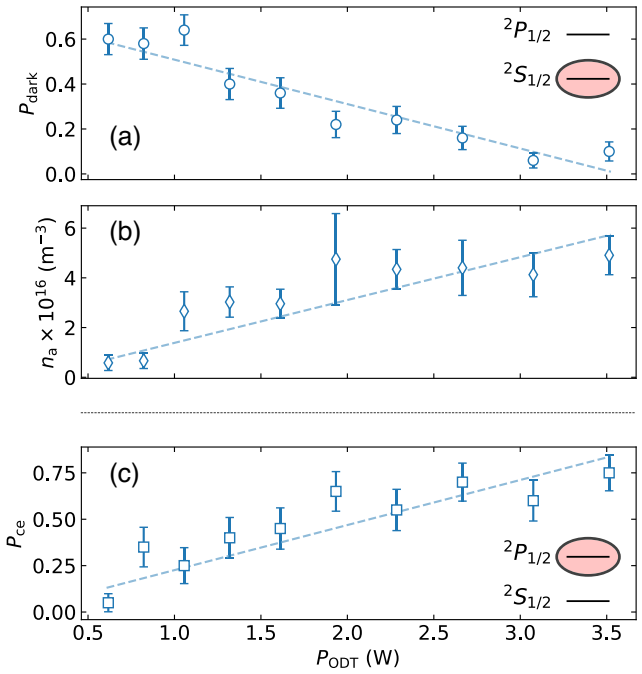

FIG. 2. Dark Yb^+ ion probability (a) as a function of the ODT power with Yb^+ initialized in $^2S_{1/2}$. Peak atom density n_a (b), obtained with time-of-flight measurements. Charge exchange probability (c) for Yb^+ in its $^2P_{1/2}$ state. The dashed lines are linear fits to the data as a guide to the eye. The error bars reflect the total statistical uncertainties.

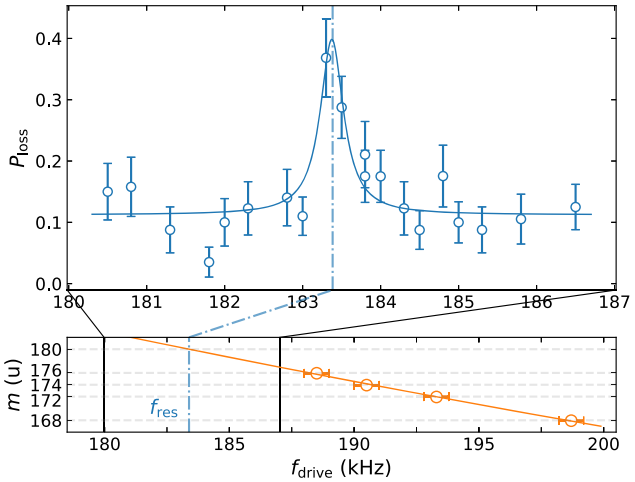

FIG. 3. Mass spectrometry of $LiYb^+$ and Yb^+ by resonant driving the radial trap frequency with f_{drive}. Top panel: ion loss (disks) with resonant driving applied during the interaction of $^{174}Yb^+$ with an ultracold mixture of $^6Li/Li_2$, with each data point corresponding to at least 57 repetitions. The solid blue line is a Lorentzian fit to the data. The dash-dotted line indicates the expected trap frequency $f_{res} \approx 183.4$ kHz for a single charged ion with mass number 180. It is obtained from frequency calibration (bottom panel) using four Yb^+ isotopes [40]. The error bars reflect the projection noise.

points towards a role of Li_2. In particular, it excludes three-body recombination of molecular ions via $Li + Li + Yb^+ \rightarrow LiYb^+ + Li$. This is supported by theory since the three-body recombination rate is given by $\Gamma_3 = k_3 n_a^2$, with coefficient $k_3 = 8\pi^2/15\sqrt{2/\mu}(2\alpha)^{5/4}E_{col}^{-3/4}$, where α is the atomic polarizability, μ is the atom-ion reduced mass and E_{col} is the collision energy [6]. For a Doppler cooled ion and our experimental parameters, $P_{ODT} = 0.9$ W, $T = 5.6(0.2)$ μK, and $n_a = 2.1(0.3) \times 10^{16}$ m^{-3}, we find $\Gamma_3 < 0.01$ s^{-1} which corresponds to the formation of one molecular ion in < 200 experimental runs. Therefore, three-body recombination of molecular ions does not play a significant role in the explored parameter space.

To further investigate the observed probability of dark events, we perform mass spectrometry to detect the presence of $LiYb^+$, as shown in Fig. 3. An rf-electric field ($f_{drive} = 180$–200 kHz) is applied to a cylindrical electrode (blue rod in Fig. 1) from which energy can be transferred to the ion motion, when f_{drive} is in resonance with the ion's radial trap frequency. When enough energy is transferred to the ion, this process leads to ion loss as the particle is heated from the trap. Since the trap frequency of the ion depends on its mass, we can use this scheme for mass spectrometry. We calibrate our system and extract the expected trap frequency f_{res} for the molecular ion $m = 180$ u by measuring the trap frequencies of various isotopes of Yb^+ [40].

Around f_{res} we find an enhancement of Yb^+ ion loss [see Fig. 3 (upper panel)], confirming that $LiYb^+$ molecular ions are formed during the interaction of the Yb^+ with the atom-dimer bath. These measurements are done by applying a 2 Vpp driving during the entire sequence and measuring ion loss ($t_c > 1500$ ms) as a function of f_{drive}. For off-resonant frequencies, photodissociation of $LiYb^+$ in the ODT beams results in dark Yb^+ ions, that mainly return within 1.5 s of Doppler cooling and thus the background Yb^+ ion loss is low. Around f_{res}, however, resonant heating moves $LiYb^+$ quickly out of the ODT beams and reduces the photodissociation probability. Thus, driving $LiYb^+$ out of the ion trap results in increased loss events. For these measurements, we prepare the atom-dimer bath at $T \approx 2$ μK and $n_a \approx 1 \times 10^{16}$ m^{-3}.

Finally, we study dimer-ion collisions in more detail by tweaking the dimer density in our system. The atomic three-body recombination rate for the process $Li + Li' + Li \rightarrow Li_2 + Li$ is a function of the atom scattering length, which can be tuned by the magnetic field B_{Li_2} in the vicinity of the 832 G Feshbach resonance. We use $P_{ODT} \approx 1.5$ W which results in $T = 5.6(2)$ μK and $n_a = 2.1(3) \times 10^{16}$ m^{-3} roughly constant over the explored magnetic field range. Note that the interactions with the ion always occur at $B = 0$ G to ensure the same binding energy during the collision with the ion.

We find significant dark ion probabilities for B_{Li_2} approaching the Feshbach resonance. The measured P_{dark} as a function of B_{Li_2} is shown as blue disks in Fig. 4(a),

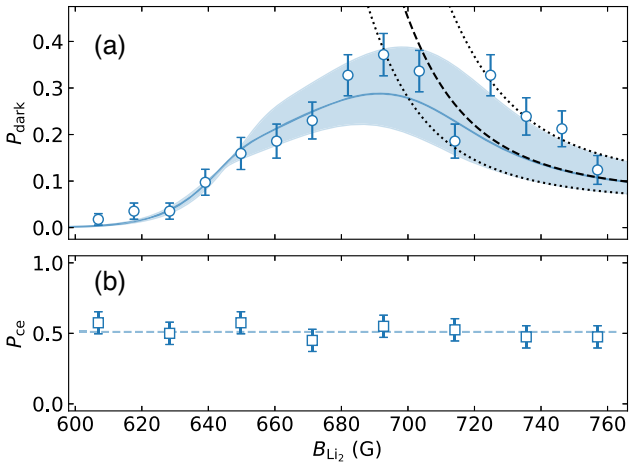

FIG. 4. (a) Dark ion and (b) charge exchange (ce) probabilities as a function of B_{Li_2}. Markers represent measurements, the black dashed line shows the simple thermal equilibrium model, and the blue solid line shows the numerical solution to rate equations. Note that no fitting parameters are used. The blue shaded region and the black dotted lines account for a 20% error in the atom temperature, typical for time-of-flight measurements. The blue dashed line in (b) shows the mean of P_{ce}. The error bars show the total statistical uncertainties.

with each data point corresponding to 40 repetitions. Below 600 G, we find negligible dark ion probabilities, in agreement with Ref. [52], whereas, when tuning B_{Li_2} above 600 G, we observe a significant increase of P_{dark}, peaking around 693 G. For comparison, we measure the charge-exchange probability to obtain a relative local atom density with the results shown in panel (b) of Fig. 4. P_{ce} is approximately constant over the explored B_{Li_2}, indicating that varying B_{Li_2} has no significant effect on the atomic density [42].

The relationship between the probability of dark ions and the magnetic field can also be calculated via the dimer density n_d. Two different approaches to obtain n_d result in the blue and the dashed black theory lines in Fig. 4(a). The dimer density is related to the probability by $P_{dark}(n_d) = 1 - e^{-\tau\lambda_d n_d}$, where $\tau = 500$ ms is the interaction time and $\lambda_d = 4.9 \times 10^{-15}$ s^{-1} m^3 is the dimer-ion Langevin collision rate per unit density. Here, we rely on the fact that every dimer-ion collision results in a molecular ion when the collision energy is much smaller than the dimer binding energy. For the presented system, this was recently demonstrated with quasiclassical trajectory simulations [41]. Moreover, the density of molecular states is much larger in the long range molecular ion potential than in the short range van der Waals potential of the dimer, i.e., it is more likely that a molecular ion is created.

The dimer density n_d as a function of the magnetic field can be calculated by looking into the three-body recombination and dissociation process that determine the dimer formation [39,40,43]. Close to the Feshbach resonance, three-body recombination of Li_2 can be described with the rate coefficient $\propto TE_b^{-3}$. This is in competition with three-body dissociation $Li_2 + Li \rightarrow Li + Li' + Li$, which has the rate coefficient $\propto T^{5/2}E_b^{-3}\exp^{-E_b/k_BT}$, where k_B is the Boltzmann constant and E_b is the dimer binding energy [39]. We obtain the binding energy for different magnetic fields B_{Li_2} using precise measurements from Ref. [37].

We find reasonable agreement with our ion-data for magnetic fields $\gtrsim$700 G, when assuming an atom-dimer thermal equilibrium to obtain the dimer density. This is shown as the black dashed line in Fig. 4. Here, the dimer density follows an analytical expression as deduced in Refs. [39,43], which we solve for the atom density and the atom temperatures of our system. However, for fields below 700 G this simple model deviates from our measurements.

We find excellent agreement with the measured data over the entire magnetic field spectrum when numerically solving the rate equations as they evolve during the evaporation ramp [40]. This results in the blue solid lines in Fig. 4. It should be stressed that there are no fitted parameters in our model. The good agreement therefore indicates that every dimer-ion collision results in a molecular ion, which subsequently dissociates to a hot Yb^+ ion, observable as a dark event in the experiment.

The results show that we can use the single ion as a sensor for Li_2 dimers in our system. In particular, we probe the local dimer density as $n_d = -\ln(1 - P_{dark})/(\tau\lambda_d)$. As an example, we consider $P_{dark} = 0.2$, which can easily be distinguished from the background (see Fig. 4). We find $n_d \approx 1 \times 10^{14}$ m^{-3} corresponding to a relative density of $n_d/n_a \approx 0.004$. Remarkably, this amounts to only about 50 Li_2 dimers in our atomic cloud and shows the potential of using trapped ions to detect trace amounts of molecular gases.

Conclusion and outlook.—We observed interactions of a single ion with ultracold Feshbach dimers and identified $Li_2 + Yb^+$ collisions as the origin for the created $LiYb^+$ in our system. We found a strong correlation between molecular ion formation and the dimer density, and observed molecular ions in our system via mass spectrometry. This is a new approach for creating molecular ions, which is independent of the mass ratio. It relies on the binding energy of the dimers being larger than the ion-dimer collision energy and the absence of strong inelastic atom-ion loss reaction channels. Atom-ion collisions and three-body recombination could be eliminated by purification of the cloud using resonant laser pulses [9]. Our results suggest the applicability of a single ion as a probe for trace molecule gases, with densities as low as 10^{14} m^{-3}. This new technique might be used to detect Feshbach molecules of various atom combinations, whose quantities are not detectable via commonly used methods [8–10].

Once the ion-dimer collision energy exceeds the Li_2 binding energy, dimer-dissociation should become prominent and reduce the molecular ion formation rate [41]. This can be simply controlled with the magnetic field during the

collision. It will be interesting to study how the collision energy, in particular the micromotion, affects the crossover between the two regimes. Feshbach dimers will allow studies of ultracold chemistry between ions and molecules, in which quantum effects such as ion-neutral Feshbach resonances [11,51] will influence the reaction channels.

We thank T. Feldker for suggesting this work, B. Pasquiou and S. Bennetts for support in exchanging the Li oven and B. Pasquiou, M. Borkowski, N. J. van Druten, and R. J. C. Spreeuw for comments on the manuscript. This work was supported by the Dutch Research Council Start-up Grant 740.018.008 (R. G.), Vrije Programma 680.92.18.05 (E. T., R. G., J. P.) and Quantum Software Consortium programme 024.003.037 (A. S. N.). R. S. L. acknowledges funding from the European Union's Horizon 2020 research and innovation programme under the Marie Sklodowska-Curie Grant No. 895473.

[1] K. Sugiyama and J. Yoda, Jpn. J. Appl. Phys. **34**, L584 (1995).
[2] K. Sugiyama and J. Yoda, Phys. Rev. A **55**, R10(R) (1997).
[3] T. M. Hoang, Y.-Y. Jau, R. Overstreet, and P. D. D. Schwindt, Phys. Rev. A **101**, 022705 (2020).
[4] R. Rugango, J. E. Goeders, T. H. Dixon, J. M. Gray, N. B. Khanyile, G. Shu, R. J. Clark, and K. R. Brown, J. Phys. **17**, 035009 (2015).
[5] S. Willitsch, M. T. Bell, A. D. Gingell, S. R. Procter, and T. P. Softley, Phys. Rev. Lett. **100**, 043203 (2008).
[6] J. P. Ríos, *An Introduction to Cold and Ultracold Chemistry* (Springer, Cham, Switzerland, 2020).
[7] B. R. Heazlewood and T. P. Softley, Nat. Rev. Chem. **5**, 125 (2021).
[8] T. Köhler, K. Góral, and P. S. Julienne, Rev. Mod. Phys. **78**, 1311 (2006).
[9] F. Ferlaino, S. Knoop, and R. Grimm, *Cold Molecules*, edited by R. Krems, B. Friedrich, and W. C. Stwalley (CRC Press, Boca Raton, 2009), Chap. 9, Ultracold Feshbach Molecules.
[10] C. Chin, R. Grimm, P. S. Julienne, and E. Tiesinga, Rev. Mod. Phys. **82**, 1225 (2010).
[11] M. Tomza, K. Jachymski, R. Gerritsma, A. Negretti, T. Calarco, Z. Idziaszek, and P. S. Julienne, Rev. Mod. Phys. **91**, 035001 (2019).
[12] L. Ratschbacher, C. Zipkes, C. Sias, and M. Köhl, Nat. Phys. **8**, 649 (2012).
[13] S. Haze, R. Saito, M. Fujinaga, and T. Mukaiyama, Phys. Rev. A **91**, 032709 (2015).
[14] S. Jyothi, T. Ray, S. Dutta, A. R. Allouche, R. Vexiau, O. Dulieu, and S. A. Rangwala, Phys. Rev. Lett. **117**, 213002 (2016).
[15] J. Joger, H. Fürst, N. Ewald, T. Feldker, M. Tomza, and R. Gerritsma, Phys. Rev. A **96**, 030703(R) (2017).
[16] L. Ratschbacher, C. Sias, L. Carcagni, J. M. Silver, C. Zipkes, and M. Köhl, Phys. Rev. Lett. **110**, 160402 (2013).
[17] T. Sikorsky, Z. Meir, R. Ben-shlomi, N. Akerman, and R. Ozeri, Nat. Commun. **9**, 920 (2018).
[18] H. Fürst, T. Feldker, N. V. Ewald, J. Joger, M. Tomza, and R. Gerritsma, Phys. Rev. A **98**, 012713 (2018).
[19] A. Härter, A. Krükow, A. Brunner, W. Schnitzler, S. Schmid, and J. H. Denschlag, Phys. Rev. Lett. **109**, 123201 (2012).
[20] J. Pérez-Ríos and C. H. Greene, J. Chem. Phys. **143**, 041105 (2015).
[21] A. Krükow, A. Mohammadi, A. Härter, and J. Hecker Denschlag, Phys. Rev. A **94**, 030701(R) (2016).
[22] A. Mohammadi, A. Krükow, A. Mahdian, M. Deiß, J. Pérez-Ríos, H. da Silva, M. Raoult, O. Dulieu, and J. Hecker Denschlag, Phys. Rev. Research **3**, 013196 (2021).
[23] C. Monroe, D. M. Meekhof, B. E. King, W. M. Itano, and D. J. Wineland, Phys. Rev. Lett. **75**, 4714 (1995).
[24] D. Leibfried, R. Blatt, C. Monroe, and D. Wineland, Rev. Mod. Phys. **75**, 281 (2003).
[25] S. Schmid, A. Härter, and J. H. Denschlag, Phys. Rev. Lett. **105**, 133202 (2010).
[26] W. Zwerger, ed., *The BCS-BEC Crossover and the Unitary Fermi Gas*, Lecture Notes in Physics Vol. 836 (Springer, Berlin Heidelberg, 2012).
[27] G. E. Astrakharchik, L. A. P. Ardila, R. Schmidt, K. Jachymski, and A. Negretti, Commun. Phys. **4**, 94 (2021).
[28] E. R. Christensen, A. Camacho-Guardian, and G. M. Bruun, Phys. Rev. Lett. **126**, 243001 (2021).
[29] L. Oghittu, M. Johannsen, A. Negretti, and R. Gerritsma, Phys. Rev. A **104**, 053314 (2021).
[30] J. Mur-Petit, J. J. García-Ripoll, J. Pérez-Ríos, J. Campos-Martínez, M. I. Hernández, and S. Willitsch, Phys. Rev. A **85**, 022308 (2012).
[31] N. B. Khanyile, G. Shu, and K. R. Brown, Nat. Commun. **6**, 7825 (2015).
[32] F. Wolf, Y. Wan, J. C. Heip, F. Gebert, C. Shi, and P. O. Schmidt, Nature (London) **530**, 457 (2016).
[33] C. wan Chou, C. Kurz, D. B. Hume, P. N. Plessow, D. R. Leibrandt, and D. Leibfried, Nature (London) **545**, 203 (2017).
[34] M. Sinhal, Z. Meir, K. Najafian, G. Hegi, and S. Willitsch, Science **367**, 1213 (2020).
[35] O. Katz, M. Pinkas, N. Akerman, and R. Ozeri, arXiv:2107.08441.
[36] H. Hirzler, T. Feldker, H. Fürst, N. V. Ewald, E. Trimby, R. S. Lous, J. D. Arias Espinoza, M. Mazzanti, J. Joger, and R. Gerritsma, Phys. Rev. A **102**, 033109 (2020).
[37] G. Zürn, T. Lompe, A. N. Wenz, S. Jochim, P. S. Julienne, and J. M. Hutson, Phys. Rev. Lett. **110**, 135301 (2013).
[38] S. Jochim, M. Bartenstein, A. Altmeyer, G. Hendl, S. Riedl, C. Chin, J. Hecker Denschlag, and R. Grimm, Science **302**, 2101 (2003).
[39] C. Chin and R. Grimm, Phys. Rev. A **69**, 033612 (2004).
[40] See Supplemental Material at http://link.aps.org/supplemental/10.1103/PhysRevLett.128.103401 for details, which contains Refs. [10,11,22,24,36,38,41–50].
[41] H. Hirzler, E. Trimby, R. S. Lous, G. C. Groenenboom, R. Gerritsma, and J. Pérez-Ríos, Phys. Rev. Research **2**, 033232 (2020).
[42] This is also confirmed by separate time-of-flight measurements of the atom density for varying B_{Li_2}.
[43] S. J. J. M. F. Kokkelmans, G. V. Shlyapnikov, and C. Salomon, Phys. Rev. A **69**, 031602(R) (2004).

[44] R. Grimm, Ultracold Fermi gases in the BEC-BCS crossover: A review from the Innsbruck perspective, in *Ultra-cold Fermi Gases*, edited by M. Inguscio, W. Ketterle, and C. Salomon (2008), *Proceedings of the International School of Physics "Enrico Fermi"* (IOP Press, Varenna, 2006), Course CLXIV.
[45] D. S. Petrov, Phys. Rev. A **67**, 010703(R) (2003).
[46] W. Ketterle and N. J. van Druten, Adv. At. Mol. Opt. Phys. **37**, 181 (1996).
[47] A. J. Moerdijk, B. J. Verhaar, and A. Axelsson, Phys. Rev. A **51**, 4852 (1995).
[48] G. F. Gribakin and V. V. Flambaum, Phys. Rev. A **48**, 546 (1993).
[49] P. S. Julienne and J. M. Hutson, Phys. Rev. A **89**, 052715 (2014).
[50] M. Bartenstein, A. Altmeyer, S. Riedl, R. Geursen, S. Jochim, C. Chin, J. H. Denschlag, R. Grimm, A. Simoni, E. Tiesinga, C. J. Williams, and P. S. Julienne, Phys. Rev. Lett. **94**, 103201 (2005).
[51] P. Weckesser, F. Thielemann, D. Wiater, A. Wojciechowska, L. Karpa, K. Jachymski, M. Tomza, T. Walker, and T. Schätz, Nature (London) **600**, 429 (2021).
[52] T. Feldker, H. Fürst, H. Hirzler, N. V. Ewald, M. Mazzanti, D. Wiater, M. Tomza, and R. Gerritsma, Nat. Phys. **16**, 413 (2020).